# Chapter 2. Jump Conditions of Shocks and Discontinuities

Shocks and discontinuities are nonlinear phenomena that are commonly observed in space plasmas. Jump conditions of one-dimensional static shocks or discontinuities can help us to identify the shocks and discontinuities from the space observations. In reality, structure of shock or discontinuity may change slowly with time and may not be a perfect plane wave. Deviations from ideal assumptions of uniform boundary condition, zero heat flux, and isotropic pressure at both upstream and downstream boundaries can also modify the resulting jump conditions. High-resolution data, multiple-satellite observations, and numerical simulations can help us to learn more about the necessity of modification on these jump conditions. Jump conditions do not provide any information on shock heating process nor fine structure in the transition region of a shock or discontinuity. The fine structure in the transition region of a discontinuity can be solved based on the pseudo-potential method, which will be discussed in the next chapter. The turbulent structures in the transition region of a shock are commonly studied by means of kinetic plasma simulations. Jump condition can help these simulations to choose their initial conditions and boundary conditions, so that these kinetic simulations can be done in a limited simulation domain.

For simplicity, we shall assume that one-dimensional steady state is a good assumption in all cases discussed in this chapter. For one-dimensional static structure, we can let $\partial/\partial t = 0$, and $\nabla = \hat{x}(d/dx)$. To obtain shock jump conditions, we are looking for structures with uniform boundary conditions. That is $d/dx \to 0$ at both upstream and downstream boundaries. Substituting uniform boundary condition into Poisson's equation yields

$\rho_c = 0$ at both upstream and downstream boundaries (2.1)

$n_i = n_e = n$ at both upstream and downstream boundaries (2.2)

Substituting static uniform boundary condition into Ampere's Law yields

$\mathbf{J} = 0$ at both upstream and downstream boundaries (2.3)

$\mathbf{V}_i = \mathbf{V}_e = \mathbf{V}$ at both upstream and downstream boundaries (2.4)

For $n_i = n_e = n$ and $\mathbf{V}_i = \mathbf{V}_e = \mathbf{V}$ at both boundaries, one can show that

$\mathbf{P} = \mathbf{P}_i + \mathbf{P}_e$ at both upstream and downstream boundaries (2.5)

$\mathbf{q} = \mathbf{q}_i + \mathbf{q}_e$ at both upstream and downstream boundaries (2.6)

**Exercise 2.1**

Show that static and uniform boundary condition yields Eq. (2.3).

**Exercise 2.2**

Show that for $n_i \approx n_e \approx n$ and $\mathbf{V}_i = \mathbf{V}_e = \mathbf{V}$, we have $\mathbf{P} = \mathbf{P}_i + \mathbf{P}_e$ and $\mathbf{q} = \mathbf{q}_i + \mathbf{q}_e$.

## 2.1. Fluid Jump Conditions of ES Shocks and Discontinuities in Unmagnetized Plasma

Basic equations of electrostatic nonlinear waves in unmagnetized plasma can be obtained from Eqs. (1.13')~(1.15'), (1.9), (1.11) and (1.16) with $\mathbf{B} = 0$ over entire space. For one-dimensional static structure, we assume $\partial/\partial t = 0$, and $\nabla = \hat{x}(d/dx)$. The fluid equations become

$$\frac{d}{dx}(\rho V_x) = 0 \tag{2.7}$$

$$\frac{d}{dx}[\rho V_x^2 + P_{xx} - \frac{\varepsilon_0 E_x^2}{2}] = 0 \tag{2.8}$$

$$\frac{d}{dx}[\rho V_x V_y + P_{xy} - \varepsilon_0 E_x E_y] = 0 \tag{2.9}$$

$$\frac{d}{dx}[\rho V_x V_z + P_{xz} - \varepsilon_0 E_x E_z] = 0 \tag{2.10}$$

$$\frac{d}{dx}[\frac{1}{2}\rho V_x^3 + \frac{3}{2}P_{xx}V_x + q_x] = 0 \tag{2.11}$$

$$\frac{d}{dx}E_x = \frac{\rho_c}{\varepsilon_0} = \frac{e(n_i - n_e)}{\varepsilon_0} \tag{2.10}$$

$$\frac{d}{dx}E_y = 0 \tag{2.11}$$

$$\frac{d}{dx}E_z = 0 \tag{2.12}$$

We look for electrostatic structures with uniform boundary conditions. That is $d/dx \to 0$ at both upstream and downstream boundaries. It yields

$\mathbf{E} = 0$. at both upstream and downstream boundaries (2.13)

For simplicity, we assume that

$P_{xy} = P_{xz} = 0$ at both upstream and downstream boundaries (2.14)

$q_x = 0$ at both upstream and downstream boundaries (2.15)

Integrating Eqs. (2.7), (2.8), and (2.9) from upstream to downstream, and making use of Eqs. (2.13), (2.14), and (2.15), we can obtain the following jump conditions

$$\rho_1 V_{x1} = \rho_2 V_{x2} \tag{2.16}$$

$$\rho_1 V_{x1}^2 + P_{xx1} = \rho_2 V_{x2}^2 + P_{xx2} \tag{2.17}$$

$$\rho_1 V_{x1} V_{y1} = \rho_2 V_{x2} V_{y2} \tag{2.18}$$

$$\rho_1 V_{x1} V_{z1} = \rho_2 V_{x2} V_{z2} \tag{2.19}$$

$$(\frac{1}{2}\rho_1 V_{x1}^2 + \frac{3}{2}P_{xx1})V_{x1} = (\frac{1}{2}\rho_2 V_{x2}^2 + \frac{3}{2}P_{xx2})V_{x2} \tag{2.20}$$

where subscripts 1 and 2 denote upstream and downstream quantities, respectively.

Example: $\int_{x=-\infty}^{x=+\infty} dx \frac{d}{dx}(\rho V_x) = [\rho V_x]_{x=-\infty}^{x=+\infty} = \rho_2 V_{x2} - \rho_1 V_{x1} = 0$ (2.21)

Substituting Eq. (2.16) into Eqs. (2.18) and (2.19) yields $V_{y1} = V_{y2}$ and $V_{z1} = V_{z2}$. For simplicity, we can choose a moving frame such that $V_{y1} = V_{y2} = 0$ and $V_{z1} = V_{z2} = 0$.

Two types of nonlinear wave solutions can be obtained from Eqs. (2.16), (2.17), and (2.20). They are (A) contact discontinuities and (B) shocks.

(A) 1-D Electrostatic Contact Discontinuity

For $V_{x1} = V_{x2} = 0$, conditions in Eqs. (2.16) and (2.21) are automatically fulfilled, whereas Eq. (2.17) can be simplified as

$$P_{xx1} = P_{xx2} \tag{2.22}$$

or

$$\rho_1 T_1 = \rho_2 T_2 \tag{2.23}$$

This is the jump condition for electrostatic (ES) Contact Discontinuity (CD). Kinetic jump condition of this electrostatic CD will be discussed in section 2.3.

(B) 1-D Electrostatic Shock

Let $C_{S1}^2 = \gamma p_1/\rho_1$, $M_{S1}^2 = V_{x1}^2/C_{S1}^2$, $x = \rho_2/\rho_1$, $y = V_{x2}/V_{x1}$, and $z = P_{xx2}/P_{xx1}$, where $V_{x1} > 0$, $\gamma = (f+2)/f = 3$, and $f = 1$ is the degree of freedom. One can obtain ES Shock jump conditions from Eqs. (2.16), (2.17), and (2.20):

$$\frac{\rho_1 V_{x1}}{\rho_1 V_{x1}} = \frac{\rho_2 V_{x2}}{\rho_1 V_{x1}} \Rightarrow$$

$$1 = xy \tag{2.24}$$

$$\frac{\rho_1 V_{x1}^{\ 2}}{P_{xx1}} + \frac{P_{xx1}}{P_{xx1}} = \frac{\rho_2 V_{x2}^{\ 2}}{P_{xx1}} + \frac{P_{xx2}}{P_{xx1}} \Rightarrow$$

$$\gamma M_{S1}^2 + 1 = \gamma M_{S1}^2 y + z \tag{2.25}$$

$$\frac{1}{2}\frac{\rho_1 V_{x1}^{\ 3}}{P_{xx1} V_{x1}} + \frac{3}{2}\frac{P_{xx1} V_{x1}}{P_{xx1} V_{x1}} = \frac{1}{2}\frac{\rho_2 V_{x2}^{\ 3}}{P_{xx1} V_{x1}} + \frac{3}{2}\frac{P_{xx2} V_{x2}}{P_{xx1} V_{x1}} \Rightarrow$$

$$\gamma M_{S1}^2 + 3 = \gamma M_{S1}^2 y^2 + 3zy \tag{2.26}$$

Equation (2.24) yields

$$x = \frac{1}{y} \tag{2.24'}$$

Equation (2.25) yields

$$z = \gamma M_{S1}^2 (1 - y) + 1 = \frac{f+2}{f} M_{S1}^2 (1 - y) + 1 \tag{2.25'}$$

Eq. (2.26) can be rewritten as

$$\frac{f+2}{f} M_{S1}^2 + (f+2) = \frac{f+2}{f} M_{S1}^2 y^2 + (f+2)zy \Rightarrow M_{S1}^2 + f = M_{S1}^2 y^2 + fzy \Rightarrow$$

$$M_{S1}^2 (1 - y^2) + f(1 - zy) = 0 \Rightarrow M_{S1}^2 (1 - y)(1 + y) + f\{1 - y[(\frac{f+2}{f} M_{S1}^2 (1 - y) + 1]\} = 0 \Rightarrow$$

$$(1 - y)\{M_{S1}^2 (1 + y) + f - y(f+2) M_{S1}^2)\} = 0 \Rightarrow (1 - y)\{M_{S1}^2 + f - y(f+1) M_{S1}^2)\} = 0 \Rightarrow$$

$y = 1$ or

$$y = \frac{1}{f+1}(\frac{f}{M_{S1}^2} + 1) \tag{2.26'}$$

where the solution of $y = 1$ is a solution of a uniform system.

For collisionless ES shock, we have $f = 1,\ \gamma = 3$ and $y = \frac{1}{2}(\frac{1}{M_{S1}^2} + 1)$.

For collisional gas dynamic shock, we have $f = 3,\ \gamma = 5/3$ and $y = \frac{1}{4}(\frac{3}{M_{S1}^2} + 1)$.

**Exercise 2.3**

Plot jump ratio *x, y,* and *z* as functions of upstream Mach number $M_{S1}$.

**Exercise 2.4**

If $T_{i1}/T_{e1} = r_1$ and $T_{i2}/T_{e2} = r_2$, determine jump conditions $z_e = (P_e)_{xx2}/(P_e)_{xx1}$ and $z_i = (P_i)_{xx2}/(P_i)_{xx1}$. Plot $z_e$ and $z_i$ as functions of upstream Mach number $M_{S1}$.

**Exercise 2.5**

(a) Let $\delta Q = (q_{x2} - q_{x1})$. Solve $y$ in terms of $M_{S1}$ and $\delta Q$.

(b) Plot your results on $y - M_{S1}$ plane for different $\delta Q$.

(c) Let $S_1$ and $S_2$ be the upstream and downstream entropy, respectively. Let $\delta S = S_2 - S_1$. Carefully examine your solutions to make sure that entropy increases across the shock ramp. Plot $\delta S$ on $\delta S - M_{S1}$ plane for different $\delta Q$.

Kinetic jump conditions (to be discussed in Section 2.3) and kinetic simulations can provide a self-consistent information on the heat flux and pressure anisotropy across the ES shock.

## 2.2. Fluid Jump Conditions of Shocks and Discontinuities in Magnetized Plasma

To study nonlinear waves in magnetized plasma, basic equations can be obtained from Eqs. $(1.6_\alpha)$~$(1.8_\alpha)$, (1.9)~(1.15), (1.13')~(1.15'), and (1.16)~(1.17). They are

$$\nabla \cdot \mathbf{E} = \frac{e(n_i - n_e)}{\varepsilon_0} = \frac{\rho_c}{\varepsilon_0} \tag{2.27}$$

$$\nabla \cdot \mathbf{B} = 0 \tag{2.28}$$

$$\nabla \times \mathbf{E} = -\frac{\partial \mathbf{B}}{\partial t} \tag{2.29}$$

$$\nabla \times \mathbf{B} = \mu_0 \mathbf{J} \tag{2.30}$$

$$\frac{\partial}{\partial t}\rho + \nabla \cdot (\rho \mathbf{V}) = 0 \tag{2.31}$$

$$\frac{\partial}{\partial t}[\rho \mathbf{V} + \frac{1}{c^2}(\frac{\mathbf{E} \times \mathbf{B}}{\mu_0})] + \nabla \cdot [\rho \mathbf{VV} + \mathbf{P} + \mathbf{1}(\frac{\varepsilon_0 E^2}{2} + \frac{B^2}{2\mu_0}) - \varepsilon_0 \mathbf{EE} - \frac{\mathbf{BB}}{\mu_0}] = 0 \tag{2.32}$$

$$\frac{\partial}{\partial t}[\frac{1}{2}\rho V^2 + \frac{3}{2}p + \frac{\varepsilon_0 E^2}{2} + \frac{B^2}{2\mu_0}] + \nabla \cdot [(\frac{1}{2}\rho V^2 + \frac{3}{2}p)\mathbf{V} + \mathbf{P} \cdot \mathbf{V} + \mathbf{q} + \frac{\mathbf{E} \times \mathbf{B}}{\mu_0}] = 0 \tag{2.33}$$

$$\frac{\partial}{\partial t}\rho_c = -\nabla \cdot [e(n_i \mathbf{V}_i - n_e \mathbf{V}_e) = -\nabla \cdot \mathbf{J} \tag{2.34}$$

$$\frac{\partial}{\partial t}\mathbf{J}+\nabla\cdot[\sum_{\alpha}(e_\alpha n_\alpha \mathbf{V}_\alpha\mathbf{V}_\alpha+\frac{e_\alpha}{m_\alpha}\mathbf{P}_\alpha)=\sum_{\alpha}(\frac{e^2n_\alpha}{m_\alpha})\mathbf{E}+\sum_{\alpha}(\frac{e^2n_\alpha\mathbf{V}_\alpha}{m_\alpha})\times\mathbf{B} \tag{2.35}$$

where $\alpha=i,e$.

For one-dimensional steady-state structure, we assume $\partial/\partial t=0$ and $\nabla=\hat{x}(d/dx)$. We look for structures with uniform boundary conditions. Namely, $d/dx\to 0$ at both upstream and downstream boundaries. Substituting uniform boundary condition into Eqs. (2.27) and (2.30) yields Eqs. (2.1)~(2.6).

Substituting static and uniform boundary conditions into Eq. (2.35) yields

$$0=\sum_{\alpha}(\frac{e^2n_\alpha}{m_\alpha})\mathbf{E}+\sum_{\alpha}(\frac{e^2n_\alpha\mathbf{V}_\alpha}{m_\alpha})\times\mathbf{B} \qquad \text{at both boundaries} \tag{2.36}$$

For $m_e<<m_i$, Eq. (2.36) can be approximated

$$\mathbf{E}=-\mathbf{V}_e\times\mathbf{B} \qquad \text{at both upstream and downstream boundaries} \tag{2.37}$$

The uniform boundary conditions yield $n_e\approx n_i=n$ and $\mathbf{V}_e\approx\mathbf{V}_i=\mathbf{V}$ at both boundaries. As a result, Eq. (2.37) can be rewritten as

$$\mathbf{E}=-\mathbf{V}\times\mathbf{B} \qquad \text{at both upstream and downstream boundaries} \tag{2.38}$$

Namely, the boundary plasma satisfies the MHD (Magnetohybrodynamic) approximation.

For $V_1<<c$ and $V_2<<c$, we have

$$\varepsilon_0E^2<<B^2/\mu_0 \qquad \text{at both upstream and downstream boundaries} \tag{2.39}$$

Under one-dimensional assumption, Eq. (2.28) yields

$$B_x=\text{constant} \qquad \text{from upstream to downstream, over entire system} \tag{2.40}$$

Two examples with different plasma boundary conditions will be discussed in this section.

*Example 1:* Plasma boundary conditions with zero heat flux and isotropic pressure

For simplicity, we assume that boundary conditions of plasma distributions are Maxwellian in velocity space. Namely, we have $\mathbf{P}_i=\mathbf{1}p_i=\mathbf{1}nk_BT_i$, $\mathbf{P}_e=\mathbf{1}p_e=\mathbf{1}nk_BT_e$, and $q_{xi}=q_{xe}=0$ at both boundaries. Substituting these boundary conditions into Eqs. (2.5) and (2.6), one can show that Eqs. (2.14) and (2.15) are also applicable to this example.

Substituting Eqs. (2.14), (2.15), (2.38), (2.39), (2.40) into Eqs. (2.29), (2.31), (2.32), (2.33) under one-dimensional and steady-state assumptions, and then integrating the resulting equations from upstream boundary to the downstream boundary, we can obtain the following jump conditions:

$$E_{y1} = E_{y2} \Rightarrow V_{x1}B_{z1} - V_{z1}B_x = V_{x2}B_{z2} - V_{z2}B_x \tag{2.41}$$

$$E_{z1} = E_{z2} \Rightarrow V_{y1}B_x - V_{x1}B_{y1} = V_{y2}B_x - V_{x2}B_{y2} \tag{2.42}$$

$$\rho_1 V_{x1} = \rho_2 V_{x2} \tag{2.43}$$

$$\rho_1 V_{x1}^2 + p_1 + \frac{B_{y1}^2 + B_{z1}^2}{2\mu_0} = \rho_2 V_{x2}^2 + p_2 + \frac{B_{y2}^2 + B_{z2}^2}{2\mu_0} \tag{2.44}$$

$$\rho_1 V_{x1} V_{y1} - \frac{B_x B_{y1}}{\mu_0} = \rho_2 V_{x2} V_{y2} - \frac{B_x B_{y2}}{\mu_0} \tag{2.45}$$

$$\rho_1 V_{x1} V_{z1} - \frac{B_x B_{z1}}{\mu_0} = \rho_2 V_{x2} V_{z2} - \frac{B_x B_{z2}}{\mu_0} \tag{2.46}$$

$$[\frac{1}{2}\rho_1 V_1^2 + \frac{5}{2}p_1]V_{x1} + (\frac{\mathbf{E}_1 \times \mathbf{B}_1}{\mu_0})_x = [\frac{1}{2}\rho_2 V_2^2 + \frac{5}{2}p_2]V_{x2} + (\frac{\mathbf{E}_2 \times \mathbf{B}_2}{\mu_0})_x \tag{2.47}$$

or

$$(\frac{1}{2}\rho_1 V_1^2 + \frac{5}{2}p_1 + \frac{B_1^2}{\mu_0})V_{x1} - (V_{x1}B_x + V_{y1}B_{y1} + V_{z1}B_{z1})\frac{B_x}{\mu_0}$$

$$= (\frac{1}{2}\rho_2 V_2^2 + \frac{5}{2}p_2 + \frac{B_2^2}{\mu_0})V_{x2} - (V_{x2}B_x + V_{y2}B_{y2} + V_{z2}B_{z2})\frac{B_x}{\mu_0} \tag{2.47a}$$

Nonlinear solutions that satisfy the above jump conditions are discussed below.

Case I: 1-D Tangential Discontinuity (TD) Solutions

For $V_{x1} = V_{x2} = 0$ and $B_x = 0$, conditions in Eqs. (2.41)~(2.43) and (2.45)~(2.47) are automatically fulfilled, and Eq. (2.44) can be simplified as

$$p_1 + \frac{B_{t1}^2}{2\mu_0} = p_2 + \frac{B_{t2}^2}{2\mu_0} \qquad \text{or} \qquad [p + \frac{B_t^2}{2\mu_0}] = 0 \tag{2.48}$$

where we use $\mathbf{B}_t = \hat{y}B_y + \hat{z}B_z$ to denote the tangential magnetic field. The notation $[A]$ denotes $[A] = A_2 - A_1$. Nonlinear structure, which satisfies Eq. (2.48), $V_{x1} = V_{x2} = 0$, $B_x = 0$, but with $\mathbf{B}_{t1} \neq \mathbf{B}_{t2}$, is called Tangential Discontinuity (TD) in MHD plasma. The tangential magnetic fields on two-sides of a TD are different either in their magnitude and/or in their direction.

Let $\mathbf{V}_t = \hat{y}V_y + \hat{z}V_z$ denote the tangential velocity field. $[\mathbf{V}_t]$ can be zero or non-zero. Strong velocity shear (i.e., $[\mathbf{V}_t] \neq 0$) on two-sides of a TD may lead to Kelvin-Helmholtz (K-H) instability, which will be discussed in Chapter 4. If there is a large angle between $\mathbf{B}_{t1}$ and $\mathbf{B}_{t2}$, a tearing mode instability may take place in the TD layer and result in magnetic reconnection.

In summary, the MHD TD satisfies the following jump conditions

$$V_n = 0 \tag{2.49a}$$

$$B_n = 0 \tag{2.49b}$$

$$[p + \frac{B_t^2}{2\mu_0}] = 0 \tag{2.49c}$$

$$[\mathbf{B}_t] \neq 0 \tag{2.49d}$$

In contrast, the tangential discontinuity in the classical gas dynamics satisfies the following jump conditions

$$V_n = 0 \tag{2.50a}$$

$$[p] = 0 \tag{2.50b}$$

$$[\mathbf{V}_t] \neq 0 \tag{2.50c}$$

Case II: 1-D Contact Discontinuity (CD) Solutions

For $V_{x1} = V_{x2} = 0$ but $B_x \neq 0$, Eqs. (2.40)-(2.47) yield the jump conditions of Contact Discontinuity (CD) in the MHD plasma. The jump conditions of the CD are summarized below.

$$V_n = 0 \tag{2.51a}$$

$$B_n \neq 0 \tag{2.51b}$$

$$[\mathbf{V}_t] = 0 \tag{2.51c}$$

$$[\mathbf{B}_t] = 0 \tag{2.51d}$$

$$[p] = 0 \tag{2.51e}$$

$$[\rho] \neq 0 \tag{2.51f}$$

$$[T] \neq 0 \tag{2.51g}$$

$$[S] \neq 0 \tag{2.51h}$$

where $S$ is the entropy of the equilibrium plasma.

Case III: 1-D Perpendicular Fast Shock Solutions

For $V_{x1} > 0$ and $B_x = 0$, and let

$$\frac{\rho_2}{\rho_1} = x, \quad \frac{V_{x2}}{V_{x1}} = y, \quad \frac{p_2}{p_1} = z$$

Eqs. (2.40)-(2.47) yield

$$xy = 1 \tag{2.52}$$

$$\frac{B_{y2}}{B_{y1}} = \frac{B_{z2}}{B_{z1}} = \frac{B_{t2}}{B_{t1}} = \frac{B_2}{B_1} = x = \frac{1}{y} \tag{2.53}$$

and

$$[\mathbf{V}_t] = 0 \tag{2.54}$$

If we choose the normal incident frame (NIF) such that $\mathbf{V}_{t1} = 0$, Eq. (2.54) yields $\mathbf{V}_{t2} = 0$. Eqs. (2.44) and (2.47) becomes

$$2M_{A1}^2 + \beta_1 + 1 = 2M_{A1}^2 y + \beta_1 z + \frac{1}{y^2} \tag{2.55}$$

$$M_{A1}^2 + \frac{5}{2}\beta_1 + 2 = (M_{A1}^2 y + \frac{5}{2}\beta_1 z + \frac{2}{y^2})y \tag{2.56}$$

where $M_{A1}^2 = \dfrac{V_{x1}^2}{B_1^2/\mu_0\rho_1}$, $\beta_1 = \dfrac{p_1}{B_1^2/2\mu_0}$.

**Exercise 2.6**

Solve Eqs. (2.55) and (2.56) to obtain $y$ and $z$ in terms of $\beta_1$ and $M_{A1}$. Choosing three different $\beta_1$, plot $y$ as a function of $M_{A1}$.

For $V_{x1} > 0$ and $B_x \neq 0$, we can multiply Eqs. (2.45) and (2.46) by $\dfrac{B_x}{\rho V_x}$. The resulting equations are

$$B_x V_{y1} - \frac{B_x^2 B_{y1}}{\mu_0\rho_1 V_{x1}} = B_x V_{y2} - \frac{B_x^2 B_{y2}}{\mu_0\rho_2 V_{x2}} \tag{2.57}$$

$$B_x V_{z1} - \frac{B_x^2 B_{z1}}{\mu_0\rho_1 V_{x1}} = B_x V_{z2} - \frac{B_x^2 B_{z2}}{\mu_0\rho_2 V_{x2}} \tag{2.58}$$

Subtracting Eqs. (2.42) from (2.57) yields,

$$V_{x1}B_{y1}(1-\frac{B_x^2}{\mu_0\rho_1V_{x1}^2})=V_{x2}B_{y2}(1-\frac{B_x^2}{\mu_0\rho_2V_{x2}^2}) \tag{2.59}$$

Summation of Eqs. (2.41) and (2.58) yields,

$$V_{x1}B_{z1}(1-\frac{B_x^2}{\mu_0\rho_1V_{x1}^2})=V_{x2}B_{z2}(1-\frac{B_x^2}{\mu_0\rho_2V_{x2}^2}) \tag{2.60}$$

Let $M_{An1}^2=\frac{V_{x1}^2}{B_x^2/\mu_0\rho_1}$ and $M_{An2}^2=\frac{V_{x2}^2}{B_x^2/\mu_0\rho_2}$. Eqs. (2.59) and (2.60) can be rewritten as

$$V_{x1}B_{y1}(1-\frac{1}{M_{An1}^2})=V_{x2}B_{y2}(1-\frac{1}{M_{An2}^2}) \tag{2.59'}$$

$$V_{x1}B_{z1}(1-\frac{1}{M_{An1}^2})=V_{x2}B_{z2}(1-\frac{1}{M_{An2}^2}) \tag{2.60'}$$

Eqs. (2.59') and (2.60') yield the following five types of solutions

Case IV: $M_{An1}^2=1$, $M_{An2}^2=1$, and $[\mathbf{B}_t]\neq 0$. It leads to the rotational discontinuity solutions.

Case V: $M_{An1}^2=1$, $M_{An2}^2\neq 1$, and $\mathbf{B}_{t2}=0$. It leads to the switch-off slow shock solutions.

Case VI: $M_{An1}^2\neq 1$, $M_{An2}^2=1$, and $\mathbf{B}_{t1}=0$. It leads to the low-beta low-Mach-number switch-on fast shock solutions.

Case VII: $B_x\neq 0$, $M_{An1}^2\neq 1$ and $M_{An2}^2\neq 1$ but $\mathbf{B}_{t1}=\mathbf{B}_{t2}=0$. It leads to gas-dynamic-like parallel shocks, including high Mach number fast shock solutions and low Mach number slow shock and intermediate shock solutions.

Case VIII: $B_x\neq 0$, $M_{An1}^2\neq 1$, $M_{An2}^2\neq 1$, $\mathbf{B}_{t1}\neq 0$ and $\mathbf{B}_{t2}\neq 0$. It leads to oblique shock solutions, including fast shock, slow shock and intermediate shock solutions.

Co-planarity Condition of Oblique Shock Solutions

For $M_{An1}^2\neq 1$ and $M_{An2}^2\neq 1$, Eqs. (2.59') and (2.60') yield

$$\frac{B_{y1}}{B_{z1}}=\frac{B_{y2}}{B_{z2}} \tag{2.61}$$

Since $\mathbf{e}_x\cdot(\mathbf{B}_1\times\mathbf{B}_2)=B_{y1}B_{z2}-B_{z1}B_{y2}$, Eq. (2.61) yields $\mathbf{e}_x\cdot(\mathbf{B}_1\times\mathbf{B}_2)=0$. That is the shock normal direction, $-\mathbf{e}_x$, and the upstream and downstream magnetic fields are co-planar.

The de-Hoffman Taylor Frame

For $V_{x1}>0$ and $B_x\neq 0$, Eqs. (2.41) and (2.42) allow us to choose a moving frame such that $\mathbf{V}_1//\mathbf{B}_1$ and $\mathbf{V}_2//\mathbf{B}_2$. Namely, $\mathbf{E}_{t1}=\mathbf{E}_{t2}=0$. This moving frame is called the

de-Hoffman-Taylor frame (dHTF). For convenience, we shall discuss the jump conditions of Cases IV~VIII based on the de-Hoffman-Taylor frame.

Case IV: 1-D Rotational Discontinuity (RD) Solutions

For $M_{An1}^2 = 1$ and $M_{An2}^2 = 1$, we have

$$V_{x1}^2 = B_x^2 / \mu_0 \rho_1 \tag{2.62a}$$

$$V_{x2}^2 = B_x^2 / \mu_0 \rho_2 \tag{2.62b}$$

Substituting Eqs. (2.62a) and (2.62b) into Eq. (2.40)-(2.47), and choose the de-Hoffman-Taylor frame, $\mathbf{E}_{t1} = \mathbf{E}_{t2} = 0$. It yields

$$\rho_1 = \rho_2 = \rho \tag{2.63}$$

$$V_{x1} = V_{x2} = V_x = \pm B_x / \sqrt{\mu_0 \rho} \tag{2.64}$$

$$\mathbf{V}_{t1} = \pm \frac{\mathbf{B}_{t1}}{\sqrt{\mu_0 \rho}} \tag{2.65a}$$

$$\mathbf{V}_{t2} = \pm \frac{\mathbf{B}_{t2}}{\sqrt{\mu_0 \rho}} \tag{2.65b}$$

$$p_1 + \frac{B_{t1}^2}{2\mu_0} = p_2 + \frac{B_{t2}^2}{2\mu_0} \tag{2.66}$$

$$\frac{B_{t1}^2}{2\mu_0} + \frac{5}{2} p_1 = \frac{B_{t1}^2}{2\mu_0} + \frac{5}{2} p_2 \tag{2.67}$$

Eqs. (2.66) and (2.67) yield $p_1 = p_2$ and $B_{t1} = B_{t2}$. A nonlinear structure, which satisfies Eqs. (2.62a)-(2.67), but with $\mathbf{B}_{t1} \neq \mathbf{B}_{t2}$, is called Rotational Discontinuity (RD). The jump condition of RD is summarized below:

$$B_n = -B_x \neq 0 \tag{2.68a}$$

$$V_x = \pm B_x / \sqrt{\mu_0 \rho} > 0 \tag{2.68b}$$

$$\mathbf{V}_t = \pm \frac{\mathbf{B}_t}{\sqrt{\mu_0 \rho}} \tag{2.68c}$$

$$[\rho] = 0 \tag{2.68d}$$

$$[V_n] = 0 \tag{2.68e}$$

$$[p] = 0 \tag{2.68f}$$

$$[B_t] = 0 \tag{2.68g}$$

but

$$[\mathbf{B}_t] \neq 0 \tag{2.68h}$$

It can be shown that entropy across an RD is constant. Therefore, structure of RD can be studied using the pseudo potential method discussed in Chapter 3.

Case V: 1-D Switch-Off Slow Shock Solutions

$M_{An1}^2 = 1,\ \ M_{An2}^2 \neq 1,$ and $\mathbf{B}_{t2} = 0.$

Case VI: 1-D Switch-On Fast Shock Solutions

$M_{An1}^2 \neq 1,\ \ M_{An2}^2 = 1,$ and $\mathbf{B}_{t1} = 0.$

Case VII: 1-D Gas-Dynamic-Like Parallel Shock Solutions

$B_x \neq 0,\ \ M_{An1}^2 \neq 1$ and $M_{An2}^2 \neq 1$ but $\mathbf{B}_{t1} = \mathbf{B}_{t2} = 0.$

Case VIII: 1-D Oblique Shock Solutions (Satisfy the Co-Planarity Condition)

$B_x \neq 0,\ \ M_{An1}^2 \neq 1,\ \ M_{An2}^2 \neq 1,\ \ \mathbf{B}_{t1} \neq 0$ and $\mathbf{B}_{t2} \neq 0$ yields $\mathbf{e}_x \cdot (\mathbf{B}_1 \times \mathbf{B}_2) = 0$. That is the shock normal direction, $-\mathbf{e}_x$, and the upstream and downstream magnetic fields are co-planar.

For simplicity, we shall choose a coordinate system such that $B_{y1} = B_{y2} = V_{y1} = V_{y2} = 0,$ and the de-Hoffman-Taylor frame such that $\mathbf{E}_{t1} = \mathbf{E}_{t2} = 0.$ The jump conditions of Case VIII (and Case V) can be obtained from Eqs. (2.40)~(2.47).

Let $\dfrac{\rho_2}{\rho_1} = x,\ \ \dfrac{V_{x2}}{V_{x1}} = y,\ \ \dfrac{p_2}{p_1} = z,$ and for $B_{z1} \neq 0,$ let $\dfrac{B_{z2}}{B_{z1}} = u$

(2.40) ➔ $B_{x1} = B_{x2} = B_x$

(2.41)➔ $E_{y1} = E_{y2} = 0 \Rightarrow V_{x1}B_{z1} - V_{z1}B_x = V_{x2}B_{z2} - V_{z2}B_x = 0 \Rightarrow \begin{bmatrix} V_{z1} = V_{x1}\dfrac{B_{z1}}{B_x} \\ V_{z2} = V_{x2}\dfrac{B_{z2}}{B_x} \end{bmatrix}$ (2.69)

(2.42)➔ $0 - 0 = 0 - 0$

(2.43)➔ $xy = 1$

(2.44)➔ $\dfrac{\rho_1 V_{x1}^2 + p_1 + \dfrac{B_{z1}^2}{2\mu_0} = \rho_2 V_{x2}^2 + p_2 + \dfrac{B_{z2}^2}{2\mu_0}}{\dfrac{B_1^2}{2\mu_0}} \Rightarrow$

$$2M_{A1}^2 + \beta_1 + \sin^2\theta_{BN1} = 2M_{A1}^2 y + \beta_1 z + \sin^2\theta_{BN1} u^2 \Rightarrow$$

$$z = 1 + \frac{1}{\beta_1}[2M_{A1}^2(1-y) + (1-\cos^2\theta_{BN1})(1-u^2)] \tag{2.70}$$

(2.45)➔ $0 - 0 = 0 - 0$

(2.46)➔ $\rho_1 V_{x1} V_{z1} - \frac{B_x B_{z1}}{\mu_0} = \rho_2 V_{x2} V_{z2} - \frac{B_x B_{z2}}{\mu_0} \Rightarrow$ (using Eq. (2.69) to eliminate $V_{z1}$ and $V_{z2}$)

$$\rho_1 V_{x1} V_{x1} \frac{B_{z1}}{B_x} - \frac{B_x B_{z1}}{\mu_0} = \rho_2 V_{x2} V_{x2} \frac{B_{z2}}{B_x} - \frac{B_x B_{z2}}{\mu_0} \Rightarrow$$

$$B_{z1}(\rho_1 V_{x1} V_{x1} - \frac{B_x B_x}{\mu_0}) = B_{z2}(\rho_2 V_{x2} V_{x2} - \frac{B_x B_x}{\mu_0}) \Rightarrow$$

$$1 - \frac{1}{M_{An1}^2} = (y - \frac{1}{M_{An1}^2})u \Rightarrow$$

$$u = \frac{1 - \frac{1}{M_{An1}^2}}{y - \frac{1}{M_{An1}^2}} \tag{2.71}$$

(Note that for Case V, $\mathbf{B}_{t2} = 0$, $M_{An1}^2 = 1$, thus $u = \frac{B_{z2}}{B_{z1}} = 0$, and (2.71) is fulfilled.)

(2.47)➔ $[\frac{1}{2}\rho_1 V_1^2 + \frac{5}{2}p_1]V_{x1} + (\frac{\mathbf{E}_1 \times \mathbf{B}_1}{\mu_0})_x = [\frac{1}{2}\rho_2 V_2^2 + \frac{5}{2}p_2]V_{x2} + (\frac{\mathbf{E}_2 \times \mathbf{B}_2}{\mu_0})_x \Rightarrow$

$$[\frac{1}{2}\rho_1(V_{x1}^2 + V_{z1}^2) + \frac{5}{2}p_1]V_{x1} = [\frac{1}{2}\rho_2(V_{x2}^2 + V_{z2}^2) + \frac{5}{2}p_2]V_{x2} \Rightarrow$$

$$[\frac{1}{2}\rho_1 V_{x1}^2(1 + \frac{B_{z1}^2}{B_x^2}) + \frac{5}{2}p_1]V_{x1} = [\frac{1}{2}\rho_2 V_{x2}^2(1 + \frac{B_{z2}^2}{B_x^2}) + \frac{5}{2}p_2]V_{x2} \Rightarrow$$

$$\left[\frac{1}{2}\rho_1 V_{x1}^3 \frac{B_1^2}{B_x^2} + \frac{5}{2}p_1 V_{x1} = \frac{1}{2}\rho_2 V_{x2}^3 \frac{B_2^2}{B_x^2} + \frac{5}{2}p_2 V_{x2}\right] \cdot \frac{B_x^2}{V_{x1} B_1^4 / 2\mu_0} \Rightarrow$$

$$M_{A1}^2 + \frac{5}{2}\beta_1 \cos^2\theta_{BN1} = M_{A1}^2 y^2 (\frac{B_2^2}{B_1^2}) + \frac{5}{2}\beta_1 \cos^2\theta_{BN1} zy \tag{2.72}$$

where

$$\frac{B_2^2}{B_1^2} = \frac{B_x^2 + B_{z2}^2}{B_1^2} = \cos^2\theta_{BN1} + \sin^2\theta_{BN1} u^2 = u^2 + \cos^2\theta_{BN1}(1-u^2) \tag{2.72a}$$

**Exercise 2.7**

(a) Show that Eqs. (2.70)~(2.72) yield the following equations for $y$:

$$(1-y)(y^3 + ay^2 + by + c) = 0$$

(b) Determine the coefficients $a$, $b$, and $c$.

(c) Choosing different $\beta_1$ and $\theta_{BN1}$, plot $y$ as a function of $M_{A1}$.

The solutions obtained in Exercise 2.7 are for $0° < \theta_{BN1} < 90°$. Only solutions with increasing entropy are acceptable solutions. When applying the solution of Exercise 2.7 to the case $\theta_{BN1} = 90°$, it gives one additional root, $y = 0$. It yields $x \to \infty$, thus it is certainly not an acceptable solution. When applying the solution of Exercise 2.7 to the case $\theta_{BN1} = 0°$, it gives one root $y = 1/M_{An1}^2 = \cos^2\theta / M_{A1}^2$. This solution is the switch-on shock solution when the upstream plasma beta and Mach number are low enough. For higher plasma beta and Mach number, this solution yields $B_{z2}^2 < 0$, thus it is not an acceptable solution in high Mach number parallel shock.

Parallel Shock

For parallel shock, $\mathbf{B}_{t1} = 0$.

Let $\frac{\rho_2}{\rho_1} = x$, $\frac{V_{x2}}{V_{x1}} = y$, $\frac{p_2}{p_1} = z$, and $\frac{B_{z2}}{B_1} = w$

(2.40) ➔ $B_{x1} = B_{x2} = B_x = B_1$

(2.41)➔ $\begin{bmatrix} V_{z1} = 0 \\ V_{z2} = V_{x2}\frac{B_{z2}}{B_x} = V_{x2}\frac{B_{z2}}{B_1} \end{bmatrix}$ (2.69')

(2.42)➔ $0 - 0 = 0 - 0$

(2.43)➔ $xy = 1$

(2.44)➔ $\dfrac{\rho_1 V_{x1}^2 + p_1 = \rho_2 V_{x2}^2 + p_2 + \frac{B_{z2}^2}{2\mu_0}}{\frac{B_1^2}{2\mu_0}} \Rightarrow \; 2M_{A1}^2 + \beta_1 = 2M_{A1}^2 y + \beta_1 z + w^2 \Rightarrow$

$$z = 1 + \frac{1}{\beta_1}[2M_{A1}^2(1-y) - w^2] \qquad (2.70')$$

(2.45)➔ $0 - 0 = 0 - 0$

(2.46)➔ $\rho_1 V_{x1} V_{z1} - \frac{B_x B_{z1}}{\mu_0} = \rho_2 V_{x2} V_{z2} - \frac{B_x B_{z2}}{\mu_0} \Rightarrow$ (using Eq. (2.69) to eliminate $V_{z1}$ and $V_{z2}$)

$$0 = \rho_1 V_{x1} V_{x2}\frac{B_{z2}}{B_1} - \frac{B_1 B_{z2}}{\mu_0} \Rightarrow$$

$$0 = B_{z2}(\rho_1 V_{x1} V_{x1}\frac{V_{x2}}{V_{x1}} - \frac{B_1^2}{\mu_0}) \Rightarrow$$

$$0 = B_{z2}\rho_1 V_{x1}^2(y - \frac{1}{M_{A1}^2})$$

Since $\rho_1 V_{x1}^2 > 0$, it yields

(a) $y = \frac{1}{M_{A1}^2}$ ` (2.71a)

(b) $B_{z2} = 0$ ` (2.71b)

(2.47)➔ $[\frac{1}{2}\rho_1 V_1^2 + \frac{5}{2}p_1]V_{x1} + (\frac{\mathbf{E}_1 \times \mathbf{B}_1}{\mu_0})_x = [\frac{1}{2}\rho_2 V_2^2 + \frac{5}{2}p_2]V_{x2} + (\frac{\mathbf{E}_2 \times \mathbf{B}_2}{\mu_0})_x \Rightarrow$

$$[\frac{1}{2}\rho_1(V_{x1}^2) + \frac{5}{2}p_1]V_{x1} = [\frac{1}{2}\rho_2(V_{x2}^2 + V_{z2}^2) + \frac{5}{2}p_2]V_{x2} \Rightarrow$$

$$[\frac{1}{2}\rho_1 V_{x1}^2 + \frac{5}{2}p_1]V_{x1} = [\frac{1}{2}\rho_2 V_{x2}^2(1 + \frac{B_{z2}^2}{B_1^2}) + \frac{5}{2}p_2]V_{x2} \Rightarrow$$

$$\left[\frac{1}{2}\rho_1 V_{x1}^3 + \frac{5}{2}p_1 V_{x1} = \frac{1}{2}\rho_2 V_{x2}^3(1 + w^2) + \frac{5}{2}p_2 V_{x2}\right] \cdot \frac{1}{V_{x1}B_1^2/2\mu_0} \Rightarrow$$

$$M_{A1}^2 + \frac{5}{2}\beta_1 = M_{A1}^2 y^2(1 + w^2) + \frac{5}{2}\beta_1 zy \quad (2.72')$$

Switch-on Shock : $\boxed{B_{z2} \neq 0 \text{ and } y = 1/M_{A1}^2}$

Substituting Eqs. (2.70') and (2.71a) into (2.72'), it yields

$$M_{A1}^2 + \frac{5}{2}\beta_1 = M_{A1}^2 \frac{1}{M_{A1}^4}(1 + w^2) + \frac{5}{2}\frac{1}{M_{A1}^2}[\beta_1 + 2M_{A1}^2(1 - y) - w^2] \Rightarrow$$

$$M_{A1}^4 + \frac{5}{2}\beta_1 M_{A1}^2 = (1 + w^2) + \frac{5}{2}[\beta_1 + 2M_{A1}^2 - 2 - w^2] \Rightarrow$$

$$M_{A1}^4 + \frac{5}{2}\beta_1 M_{A1}^2 = \frac{5}{2}\beta_1 + 5M_{A1}^2 - 4 - \frac{3}{2}w^2 \Rightarrow$$

$$w^2 = -\frac{8}{3} - \frac{2}{3}M_{A1}^4 + \frac{5}{3}\beta_1(1 - M_{A1}^2) + \frac{10}{3}M_{A1}^2$$

Only a limited range of $M_{A1}^2$ and $\beta_1$ can yield $w^2 > 0$. It can be shown that, for $M_{A1}^2 > 1$,

$w^2 > 0$➔ $+\frac{5}{2}\beta_1(1 - M_{A1}^2) > (M_{A1}^2 - 1)(M_{A1}^2 - 4) \Rightarrow$

$$M_{A1}^2 < 4 - \frac{5}{2}\beta_1$$

For $\beta_1 = 0$, it yields the switch on shock can be found when $1 < M_{A1} < 2$

For $M_{A1}^2 > 1$, it yields $\frac{5}{6}\beta_1 < 1$ or $\frac{\gamma}{2}\beta_1 = \frac{C_{S1}^2}{C_{A1}^2} < 1$ is one of the necessary conditions for the

existence of the switch-on shock solution. Namely, there is no switch-on shock solution if $C_{S1}^2 > C_{A1}^2$.

Gas-Dynamic-Like Parallel Shock: $\boxed{B_{z2} = 0}$

$B_{z2} = 0 \Rightarrow w^2 = 0$

(2.70') $\Rightarrow$ $z = 1 + \frac{1}{\beta_1}[2M_{A1}^2(1-y)]$, (2.70")

(2.72') $\Rightarrow$ $M_{A1}^2 + \frac{5}{2}\beta_1 = M_{A1}^2 y^2 + \frac{5}{2}\beta_1 zy$ (2.72")

Substituting Eqs. (2.70") and into (2.72"), it yields

$$M_{A1}^2 + \frac{5}{2}\beta_1 = M_{A1}^2 y^2 + \frac{5}{2}y[\beta_1 + 2M_{A1}^2(1-y)] \Rightarrow$$

$$M_{A1}^2(1-y^2) + \frac{5}{2}(1-y)\beta_1 - 5M_{A1}^2(1-y)y = 0 \Rightarrow$$

$$M_{A1}^2(1+y) + \frac{5}{2}\beta_1 - 5M_{A1}^2 y = 0 \Rightarrow$$

$$y = \frac{1}{4} + \frac{5}{8}\frac{\beta_1}{M_{A1}^2}$$

For $y < 1$, it yields $\frac{5}{6}\beta_1 < M_{A1}^2$ or $V_{x1} > C_{S1}$

Substituting $y = \frac{1}{4} + \frac{5}{8}\frac{\beta_1}{M_{A1}^2}$ into equation (2.70"), it yields

$$z = \frac{3}{2}\frac{M_{A1}^2}{\beta_1} - \frac{1}{4}$$

The solution of Case VI and Case VII are summarized below

Case VI: 1-D Switch-On Fast Shock (Low-Mach Number Parallel Fast Shock)

$B_x \neq 0$, $\mathbf{B}_{t1} = 0$, $M_{An1}^2 = M_{A1}^2 \neq 1$, $M_{An2}^2 = 1$, and $\mathbf{B}_{t2} \neq 0$

$$y = \frac{V_{x2}}{V_{x1}} = \frac{1}{M_{A1}^2}$$

$$1 < M_{A1}^2 < 4 - \frac{5}{2}\beta_1$$

$$C_{S1}^2 > C_{A1}^2 \quad \text{or} \quad \frac{5}{6}\beta_1 < 1$$

$$w^2 = \frac{B_{z2}^2}{B_1^2} = -\frac{8}{3} - \frac{2}{3}M_{A1}^4 + \frac{5}{3}\beta_1(1 - M_{A1}^2) + \frac{10}{3}M_{A1}^2$$

$$z = \frac{p_2}{p_1} = 1 + \frac{1}{\beta_1}[2M_{A1}^2(1-y) - w^2]$$

Case VII: 1-D Gas-Dynamic-Like Parallel Shock

$B_x \neq 0$, $\mathbf{B}_{t1} = \mathbf{B}_{t2} = 0$, $M_{An1}^2 = M_{A1}^2 \neq 1$, and $M_{An2}^2 = M_{A2}^2 \neq 1$.

$$y = \frac{V_{x2}}{V_{x1}} = \frac{1}{4} + \frac{5}{8}\frac{\beta_1}{M_{A1}^2}$$

$$w^2 = \frac{B_{z2}^2}{B_1^2} = 0$$

$$[\mathbf{B}] = [B_x] = 0$$

$$z = \frac{p_2}{p_1} = \frac{3}{2}\frac{M_{A1}^2}{\beta_1} - \frac{1}{4}$$

$$\frac{5}{6}\beta_1 < M_{A1}^2 \quad \text{or} \quad V_{x1} > C_{S1}$$

Let us define the curves $y = (1/4) + (5/8)(\beta_1 / M_{A1}^2)$ and $y = 1/M_{A1}^2$ to be Curves I and II, respectively. The intersection of the two curves is located at $M_{A1}^2 = 4 - (5\beta_1/2)$. For Curve I, solutions on the right-hand side of the intersection point correspond to the fast shock solutions. Solutions on the left-hand side of the intersection point include the slow shock solutions and the intermediate shock solutions. For Curve II, solutions on the right-hand side of the intersection point are unacceptable solutions. Solutions on the left-hand side of the intersection point are the switch-on fast shock solutions. (See Figure 2.3a) The intersection point does not exist when $C_{S1} > C_{A1}$.

It can be shown that solutions obtained from Eqs. (2.70)-(2.72) include fast shock, slow shock, fast-Alfven-slow shock, fast-Alfven shock, Alfven shock, and Alfven-slow shock. Definition of these shocks are given in Table 2.1 and Figure 2.1, where $V_{FA1}$, $V_{AX1}$, and $V_{SL1}$ are upstream fast-mode speed, Alfven-mode speed, and slow-mode speed, respectively. $V_{FA2}$, $V_{AX2}$, and $V_{SL2}$ are downstream fast-mode speed, Alfven-mode speed, and slow-mode speed, respectively. Examples of solution space of intermediate shocks (i.e., fast-Alfven-slow shock, fast-Alfven shock, Alfven shock, and Alfven-slow shock) are shown in Figure 2.2. Examples of solution $y = V_{x2}/V_{x1}$ as function of upstream Mach number

$M_{A1}$ is given in Figure 2.3. Jump conditions obtained from Eqs. (2.40)~(2.47) are also called Rankine-Hugoniot (R-H) relation.

**Table 2.1** Upstream and downstream normal flow speed of MHD shock waves

| Shock Types | Brief Notations | Upstream Flow Speed | Downstream Flow Speed |
|---|---|---|---|
| Fast | $1 \rightarrow 2$ | $V_{F1} < V_{N1}$ | $V_{AX2} < V_{N2} < V_{F2}$ |
| Fast-Alfvén | $1 \rightarrow 3$ | $V_{F1} < V_{N1}$ | $V_{SL2} < V_{N2} < V_{AX2}$ |
| Fast-Alfvén-Slow | $1 \rightarrow 4$ | $V_{F1} < V_{N1}$ | $V_{N2} < V_{SL2}$ |
| Alfvén | $2 \rightarrow 3$ | $V_{AX1} < V_{N1} < V_{F1}$ | $V_{SL2} < V_{N2} < V_{AX2}$ |
| Alfvén-Slow | $2 \rightarrow 4$ | $V_{AX1} < V_{N1} < V_{F1}$ | $V_{N2} < V_{SL2}$ |
| Slow | $3 \rightarrow 4$ | $V_{SL1} < V_{N1} < V_{AX1}$ | $V_{N2} < V_{SL2}$ |

$V_{N1}$ is the normal upstream flow speed in the shock rest frame.
$V_{N2}$ is the normal downstream flow speed in the shock rest frame.
Brief notations are obtained based on upstream and downstream states of each shock and the corresponding areas shown in Figure 2.1.

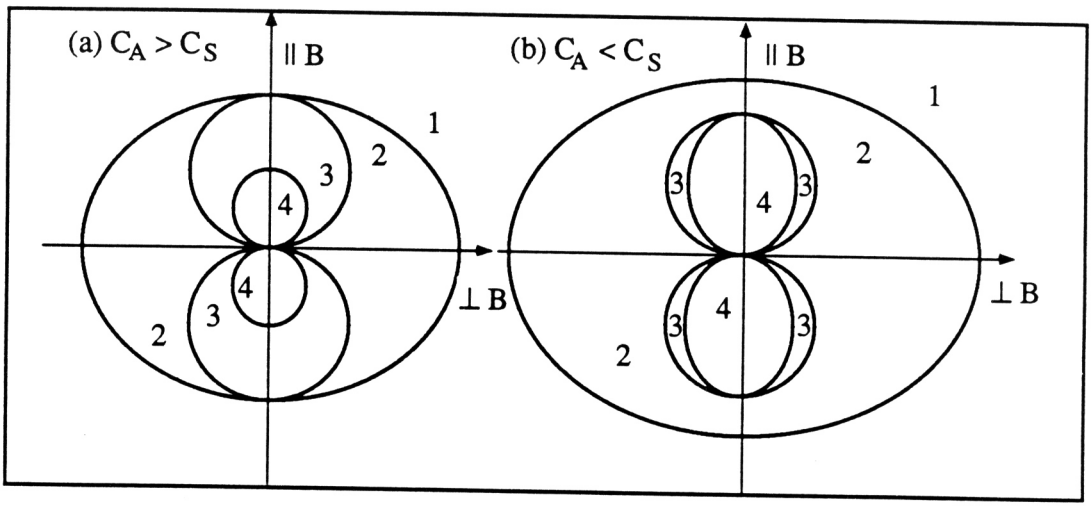


**Figure 2.1** Friedrichs' diagrams of MHD waves with (*a*) $C_A > C_S$ and (*b*) $C_A < C_S$. The Friedrichs' diagram displays the dependence of three MHD wave phase speeds (radial coordinate) on their angle of propagation with respect to the ambient magnetic field (the angular coordinate measured from the vertical axis). MHD shock waves can be found with upstream state in areas 1, 2, and 3 and with downstream state in areas 2, 3, and 4 as listed in Table **2.1.**

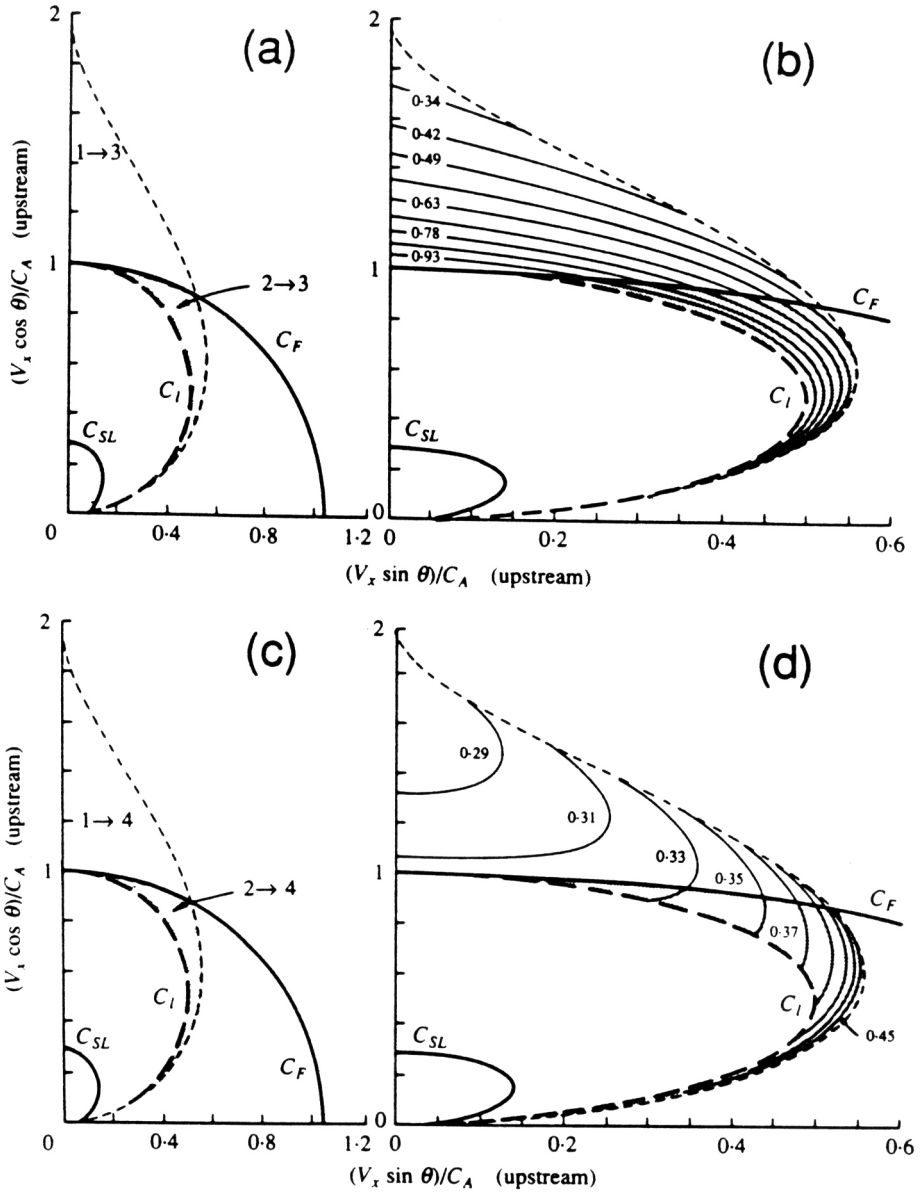


**Figure 2.2** Solution space and velocity contrast across the intermediate shock in Friedrichs' diagram format for a $\beta = 0.1$ plasma. These diagrams are reproduced from *Kennel et al.* [1989], where diagrams (*b*) and (*d*) are plotted in an expended scale of diagrams (*a*) and (*c*), respectively. $\theta$ denotes the shock normal angle. Notations $C_F$, $C_I$, and $C_{SL}$ are the same as notations $V_F$, $V_{AX}$, and $V_{SL}$ used in this chapter. Notations $1 \rightarrow 3$, $1 \rightarrow 4$, $2 \rightarrow 3$ and $2 \rightarrow 4$ are the same as defined in Table 3.1. Thus, the solution space shown in diagrams (*a*) and (*b*) denotes a smooth transition from fast-Alfvén shock to Alfvén shock. The solution space shown in diagrams (*c*) and (*d*) denotes a smooth transition from fast-Alfvén-slow shock to Alfvén-slow shock.

[Kennel, C. F., R. D. Blandford, and P. Coppi, MHD intermediate shock discontinuities. Part 1. Rankine-Hugoniot conditions, *J. Plasma Phys., 42,* 299, 1989.]

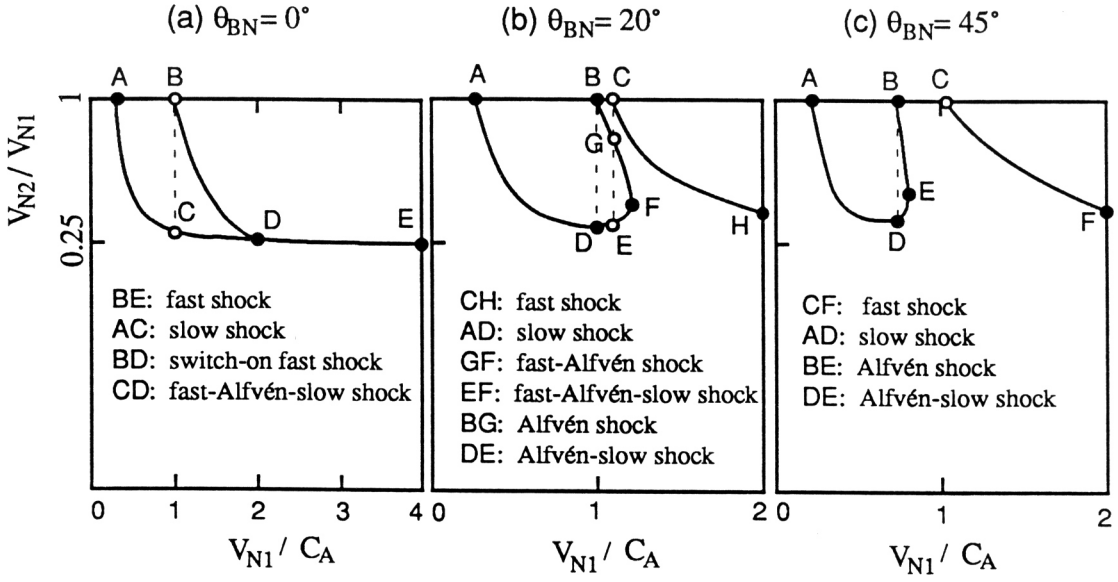


**Figure 2.3** Velocity jump across various types of MHD shocks for $\beta = 0.1$, $\theta_{BN} =$ (*a*) 0°, (*b*) 20° and (*c*) 45°, where $V_{N1}$ and $V_{N2}$ are the upstream and downstream normal flow speed in the shock rest frame, respectively.

**Exercise 2.8**

Let $y = V_{x2}/V_{x1}$ $\beta_1 = p_1/(B_1^2/2\mu_0)$, obtain jump conditions of $y$ as a function of $M_{A1}$ for different $\theta_{BN1}$ and $\beta_1$.

Consider the following cases:

$(\theta_{BN1},\beta_1) = (0°,0.1),(20°,0.1),(45°,0.1),(15°,2),(75°,2)$.

Plot solutions $V_{x2}/V_{x1}$, $\rho_2/\rho_1$, $p_2/p_1$, $B_2/B_1$, $S_2 - S_1$, $V_{x1}/V_{FA1}$, $V_{x1}/V_{AX1}$, $V_{x1}/V_{SL1}$, $V_{x2}/V_{FA2}$, $V_{x2}/V_{AX2}$, $V_{x2}/V_{SL2}$, as functions of $M_{A1}$ for each case and determine solution types to be fast shock, or slow shock, or Alfven shock, or Alfven-slow shock, or fast-Alfven shock, or fast-Alfven-slow shock, or any other type of solutions. Compare your results with solutions shown in Figure 2.3.

*Example 2:* Plasma boundary condition with non-zero heat flux and anisotropic pressure

Jump conditions of RDs and Shocks can also be generalized to include both pressure-anisotropy and heat-flux effects. In this example, we assume that

$$\mathbf{P} \approx \mathbf{bb}p_{\parallel} + (\mathbf{1} - \mathbf{bb})p_{\perp} \quad \text{at both upstream and downstream boundaries} \tag{2.73}$$

where $\mathbf{b} = \mathbf{B}/B$ denotes the unit vector along the local magnetic field. By definition, the scalar pressure is

$$p = \frac{1}{3}\text{trace}(\mathbf{P}) = \frac{1}{3}(p_{\parallel} + 2p_{\perp}) \tag{2.74}$$

For convenience, we shall define an anisotropy parameter

$$\xi = 1 - \frac{p_{\parallel} - p_{\perp}}{B^2/\mu_0} \tag{2.75}$$

Substituting Eq. (2.75) into Eq. (2.73) yields,

$$\mathbf{P} \approx \mathbf{1}p_{\perp} + (1-\xi)\frac{\mathbf{BB}}{\mu_0} \qquad \text{at both upstream and downstream boundaries} \tag{2.76}$$

Solving Eqs. (2.74) and (2.75) yields,

$$p_{\perp} = p - \frac{1}{3}(1-\xi)\frac{B^2}{\mu_0} \tag{2.77}$$

and

$$p_{\perp} + \frac{B^2}{2\mu_0} = p + \frac{1}{3}(\xi + \frac{1}{2})\frac{B^2}{\mu_0} \tag{2.78}$$

Substituting Eqs. (2.76) and (2.38)~(2.40) into Eqs. (2.32) and (2.33) yields

$$\frac{\partial}{\partial t}(\rho\mathbf{V}) + \nabla\cdot[\rho\mathbf{VV} + \mathbf{1}(p_{\perp} + \frac{B^2}{2\mu_0}) - \xi\frac{\mathbf{BB}}{\mu_0}] = 0 \tag{2.79}$$

$$\frac{\partial}{\partial t}[\frac{\rho V^2}{2} + \frac{3p}{2} + \frac{B^2}{2\mu_0}] + \nabla\cdot[(\frac{\rho V^2}{2} + \frac{3p}{2} + \frac{B^2}{\mu_0})\mathbf{V} + p_{\perp}\mathbf{V} - \xi\frac{\mathbf{BB}}{\mu_0}\cdot\mathbf{V} + \mathbf{q}] = 0 \tag{2.80}$$

or

$$\frac{\partial}{\partial t}[\frac{\rho V^2}{2} + \frac{3p_{\perp}}{2} + \frac{2-\xi}{2}\frac{B^2}{\mu_0}] + \nabla\cdot[(\frac{\rho V^2}{2} + \frac{5p_{\perp}}{2} + \frac{3-\xi}{2}\frac{B^2}{\mu_0})\mathbf{V} - \xi\frac{\mathbf{BB}}{\mu_0}\cdot\mathbf{V} + \mathbf{q}] = 0 \tag{2.81}$$

Substituting Eqs. (2.77) and (2.78) into Eqs. (2.79) and (2.80) yields

$$\frac{\partial}{\partial t}(\rho\mathbf{V}) + \nabla\cdot[\rho\mathbf{VV} + \mathbf{1}(p + \frac{2\xi+1}{3}\frac{B^2}{2\mu_0}) - \xi\frac{\mathbf{BB}}{\mu_0}] = 0 \tag{2.82}$$

$$\frac{\partial}{\partial t}[\frac{\rho V^2}{2} + \frac{3p}{2} + \frac{B^2}{2\mu_0}] + \nabla\cdot[(\frac{1}{2}\rho V^2 + \frac{5}{2}p + \frac{2+\xi}{3}\frac{B^2}{\mu_0})\mathbf{V} - \xi\frac{\mathbf{BB}}{\mu_0}\cdot\mathbf{V} + \mathbf{q}] = 0 \tag{2.83}$$

Integrating Eqs. (2.79) and (2.81) from upstream to downstream, under one-dimensional steady-state assumption, yields

$$\rho_1 V_{x1}^2 + (p_{\perp 1} + \frac{B_1^2}{2\mu_0}) - \xi_1\frac{B_x^2}{\mu_0} = \rho_2 V_{x2}^2 + (p_{\perp 2} + \frac{B_2^2}{2\mu_0}) - \xi_2\frac{B_x^2}{\mu_0} \tag{2.84}$$

$$\rho_1 V_{x1}V_{y1} - \xi_1\frac{B_x B_{y1}}{\mu_0} = \rho_2 V_{x2}V_{y2} - \xi_2\frac{B_x B_{y2}}{\mu_0} \tag{2.85}$$

$$\rho_1 V_{x1} V_{z1} - \xi_1 \frac{B_x B_{z1}}{\mu_0} = \rho_2 V_{x2} V_{z2} - \xi_2 \frac{B_x B_{z2}}{\mu_0} \tag{2.86}$$

$$\left(\frac{\rho_1 V_1^2}{2} + \frac{5p_{\perp 1}}{2} + \frac{3-\xi_1}{2}\frac{B_1^2}{\mu_0}\right)V_{x1} - \xi_1 \frac{V_{x1}B_x + V_{y1}B_{y1} + V_{z1}B_{z1}}{\mu_0} B_x + q_{x1}$$

$$= \left(\frac{\rho_2 V_2^2}{2} + \frac{5p_{\perp 2}}{2} + \frac{3-\xi}{2}\frac{B_2^2}{\mu_0}\right)V_{x2} - \xi_2 \frac{V_{x2}B_x + V_{y2}B_{y2} + V_{z2}B_{z2}}{\mu_0} B_x + q_{x2} \tag{2.87}$$

According to Eqs. (2.82) and (2.83), we can rewrite Eqs. (2.84) and (2.87) in the following forms.

$$\rho_1 V_{x1}^2 + p_1 + \frac{2\xi_1 + 1}{3}\frac{B_1^2}{2\mu_0} - \xi_1 \frac{B_x^2}{\mu_0} = \rho_2 V_{x2}^2 + p_2 + \frac{2\xi_2 + 1}{3}\frac{B_2^2}{2\mu_0} - \xi_2 \frac{B_x^2}{\mu_0} \tag{2.84'}$$

$$\left(\frac{\rho_1 V_1^2}{2} + \frac{5p_1}{2} + \frac{\xi_1 + 2}{3}\frac{B_1^2}{\mu_0}\right)V_{x1} - \xi_1 \frac{V_{x1}B_x + V_{y1}B_{y1} + V_{z1}B_{z1}}{\mu_0} B_x + q_{x1}$$

$$= \left(\frac{\rho_2 V_2^2}{2} + \frac{5p_2}{2} + \frac{\xi_2 + 2}{3}\frac{B_2^2}{\mu_0}\right)V_{x2} - \xi_2 \frac{V_{x2}B_x + V_{y2}B_{y2} + V_{z2}B_{z2}}{\mu_0} B_x + q_{x2} \tag{2.87'}$$

For $V_{x1}^2 = \xi_1 B_x^2/\mu_0\rho_1$ and $V_{x2}^2 = \xi_2 B_x^2/\mu_0\rho_2$, RD type of solutions can be obtained from Eqs. (2.41)~(2.43) and (2.84)~(2.87). Likewise, for $V_{x1}^2 \neq \xi_1 B_x^2/\mu_0\rho_1$ and $V_{x2}^2 \neq \xi_2 B_x^2/\mu_0\rho_2$, shock type of solutions can be obtained from Eqs. (2.41)~(2.43) and (2.84)~(2.87') with three vectors, shock normal $\mathbf{n} = -\hat{x}$, upstream magnetic field $\mathbf{B}_1$, and downstream magnetic field $\mathbf{B}_2$, lying on the same plane.

**Exercise 2.9**

Read the following papers. Derive RD and Shock jump conditions shown in these papers from Eqs. (2.41)~(2.43) and (2.84)~(2.87') with anisotropic pressure and non-zero heat flux.

Chao, J. K., Interplanetary collisionless shock waves, *Rep. CSR TR-70-3,* MIT Center for Space Research, Cambridge, Mass., 1970.

Chao, J. K., and B. Goldstein, Modification of the Rankine-Hugoniot relations for shocks in space, *J. Geophys. Res., 77*, 5455, 1972.

Hudson, P. D., Discontinuities in an anisotropic plasma and their identification in the solar wind, *Planet. Space Sci., 18,* 1611, 1970.

Lyu, L. H., and J. R. Kan, Shock jump conditions modified by pressure anisotropy and heat flux for Earth's bowshock, *J. Geophys. Res., 91*, 6771, 1986.

**Exercise 2.10**

Give a few examples to demonstrate modifications on jump conditions of shocks and RDs, due to presence of pressure anisotropy and non-zero heat flux at upstream and downstream boundaries.

**Exercise 2.11**

Show that for a perfect bi-Maxwellian distribution function, its pressure tensor can be written as $\mathbf{P} = \mathbf{bb}p_{\parallel} + (\mathbf{1} - \mathbf{bb})p_{\perp}$ but with zero heat flux (i.e., $\mathbf{q} = 0$).

**Exercise 2.12**

Make a table to summarize jump conditions obtained in Sections 2.1 and 2.2.

## 2.3. Kinetic Jump Conditions

In fluid jump conditions, ion-electron temperature ratio, pressure anisotropy, heat-flux difference, or potential difference are free parameters. In kinetic jump conditions, these parameters must be obtained self-consistently from steady-state Vlasov equations with $\nabla = \hat{x}(\partial/\partial x)$.

Let us consider the simplest example: ES nonlinear structure in unmagnetized plasma. For 1-D electrostatic nonlinear waves, Poisson equation can be written as

$$\frac{d^2\Phi}{dx^2} = \frac{-1}{\varepsilon_0}\sum_{\alpha}\int e_\alpha F_\alpha dv_x = -e(n_i - n_e) \tag{2.88}$$

where $F_\alpha = F_\alpha(v_x, x) = \iint f_\alpha(v_x, v_y, v_z, x)dv_y dv_z$ and $f_\alpha$ is distribution function of the $\alpha$th species. Let $F_\alpha$ satisfies electrostatic steady-state Vlasov equation, i.e.,

$$v_x\frac{\partial F_\alpha}{\partial x} - \frac{e_\alpha}{m_\alpha}\frac{d\Phi(x)}{dx}\frac{\partial F_\alpha}{\partial v_x} = 0 \tag{2.89}$$

Solution of Eq. (2.89) is

$$F_\alpha = F_\alpha\left(v_x^2 + \frac{2e_\alpha\Phi(x)}{m_\alpha}\right) \tag{2.90}$$

where $m_\alpha v_x^2 + 2e_\alpha\Phi(x) = \text{constant}$ is a characteristic curve of Eq. (2.89). Distribution function $F_\alpha$, which satisfies Eq. (2.89), keeps a constant value along a characteristic curve.

For a given $\Phi(x)$ profile, the characteristic curves in the phase space $(x, v_x)$ are well determined.

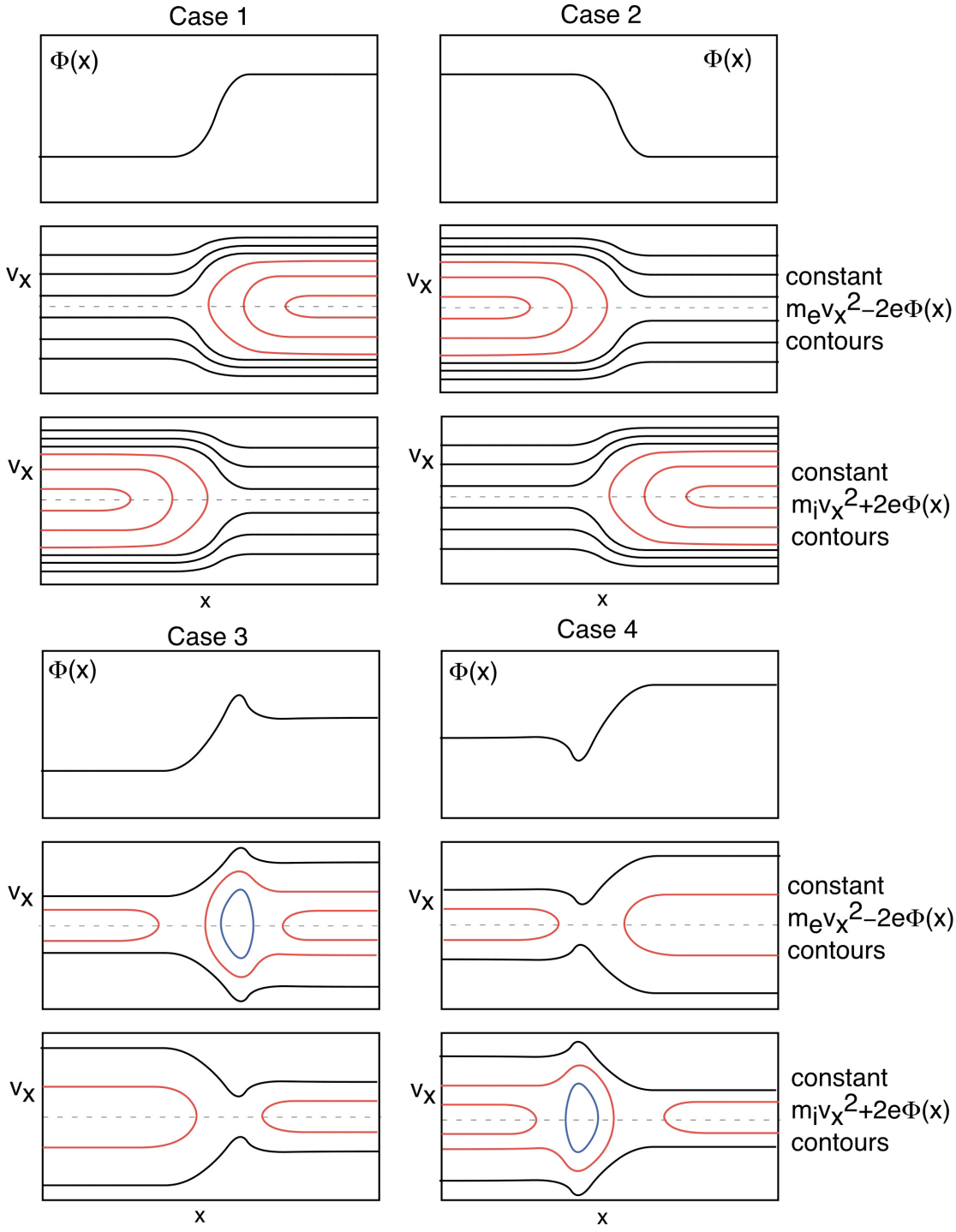


**Figure 2.4** Sketches of $\Phi(x)$ profiles and the corresponding characteristic curves $m_i v_x^2 + 2e\Phi(x) = \text{constant}$ and $m_e v_x^2 - 2e\Phi(x) = \text{constant}$ in phase space $(v_x, x)$. See text for detail discussion.

Figure 2.4 sketches examples of $\Phi(x)$ profiles and the corresponding characteristic curves $m_i v_x^2 + 2e\Phi(x) = \text{constant}$ and $m_e v_x^2 - 2e\Phi(x) = \text{constant}$ in phase space $(v_x, x)$. They are three types of characteristic curves. Type-I characteristic curves (black curves) connect upstream and downstream boundaries. These curves denote trajectory of transmitted particles. Type-II characteristic curves (red curves) connect from one part of velocity space back to another part of velocity space at the same boundary. These curves denote trajectory of reflected particles. Type-III characteristic curves (blue curves) form an island in the phase space. These curves denote trajectory of wave-trapped particles.

Let $x \to -\infty$ denotes upstream boundary and $x \to +\infty$ denotes downstream boundary. For one-dimensional steady-state structure with uniform boundary conditions, Poisson equation yields zero charge density at both upstream and downstream boundaries. Namely

$$\int F_i(x \to +\infty, v_x) dv_x = \int F_e(x \to +\infty, v_x) dv_x \tag{2.91}$$

$$\int F_i(x \to -\infty, v_x) dv_x = \int F_e(x \to -\infty, v_x) dv_x \tag{2.92}$$

For one-dimensional steady-state Ampere's law, Eq. (2.12) yields zero electric current density. That is

$$\int v_x F_i(x, v_x) dv_x = \int v_x F_e(x, v_x) dv_x \tag{2.93}$$

It can be shown that particle flux is conserved along each characteristic curve. Thus, if boundary distributions satisfy Eq. (2.93) then the entire system shall satisfy Eq. (2.93). Thus, for kinetic jump conditions, we look for boundary conditions that satisfy Eqs. (2.91), (2.92), and satisfy

$$\int v_x F_i(x \to +\infty, v_x) dv_x = \int v_x F_e(x \to +\infty, v_x) dv_x \tag{2.94}$$

$$\int v_x F_i(x \to -\infty, v_x) dv_x = \int v_x F_e(x \to -\infty, v_x) dv_x \tag{2.95}$$

Eqs. (2.90), (2.91), (2.92), (2.94), and (2.95), are kinetic jump conditions of $\Phi$, $F_i$, and $F_e$. It can be seen from Figure 2.4 that overshoot or undershoot structure on $\Phi(x)$ profile can affect solution of the jump conditions.

Since ion-electron temperature ratio, heat flux, and pressure anisotropy can be obtained from $F_i$, and $F_e$, jump conditions on these quantities become well determined. The assumption of Maxwellian distributions at upstream and downstream boundaries, commonly used in fluid jump conditions, can make one characteristic curve of $F_\alpha$ with different $F_\alpha$ values at two ends of the curve. Thus, to satisfy the assumption of Maxwellian distributions at upstream

and downstream boundaries may require a highly time-dependent transition region.

Kinetic jump conditions given in Eqs. (2.90), (2.91), (2.92), (2.94), and (2.95) are applicable to electrostatic contact discontinuities and low Mach number ES shocks. For very high Mach number shocks, turbulent structures in shock transition region usually show strong time-dependent variations. For time-dependent turbulent transition region, particles' trajectories may switch between the ones shown in Cases 1, 2, and 3. The final destination of a particle will depend on the structure of $\Phi(x,t)$ in the transition region when this particle arrives the shock transition region. Thus, even if $\Phi(x \to -\infty)$ and $\Phi(x \to -\infty)$ are static, we still cannot make a perfect prediction on particle trajectories nor distribution functions at upstream and downstream boundaries.

Application of the kinetic jump condition discussed in this section is particularly useful when we try to determine plasma jump condition of a contact discontinuity. It can be easily shown from Figure 2.4 that if there is a potential jump across a CD, then ion-electron temperature ratio at upstream boundary should not be the same as it at downstream boundary. This result predicts that, for a given ion-electron temperature ratio on both upstream and downstream boundaries, no steady contact discontinuity can be found in a full-particle-code simulation.

**Exercise 2.13**

Read the following papers, which study CDs' structures by means of plasma simulations. Show that the initial conditions and boundary conditions used in their simulations do not satisfy the kinetic jump condition of a steady-state contact discontinuity.

Wu, B. H., J. K. Chao, W. H. Tsai, Y. Lin, and L. C. Lee, A hybrid simulation of contact discontinuity, *Geophys. Res. Lett., Vol. 21,* No. 18, pp. 2059-2062, 1994.

Lapenta, G., and J. U. Brackbill, Contact discontinuities in collisionless plasmas: A comparison of hybrid and kinetic simulations, *Geophys. Res. Lett. Vol. 23,* No. 14, pp. 1713-1716, 1996.